International Journal of Applied Pharmaceutics

ISSN- 0975-7058 Vol 14, Special Issue 3, 2022

Original Article

IDENTIFICATION AND AUTHENTICATION OF HONEY USING CHEMOMETRIC ANALYSIS BASED ON ATR-FTIR AND RAMAN SPECTROSCOPY

MUHAMAD SAHLAN[1,2*], NUR ANNISA LUTHFIYAH AHLAM[1], ALI AGUS[3], ARDO SABIR[4], DIAH KARTIKA PRATAMI[5]

[1]Department of Chemical Engineering, Faculty of Engineering, Universitas Indonesia, Depok, West Java, 16424, Indonesia, [2]Research Center for Biomedical Engineering, Faculty of Engineering, Universitas Indonesia, Depok, West Java, 16424, Indonesia, [3]Faculty of Animal Science, Universitas Gadjah Mada, Yogyakarta, 55281, Indonesia, [4]Department of Conservative Dentistry, Faculty of Dentistry, Hasanuddin University, Makassar, South Sulawesi, 90245, Indonesia, [5]Lab of Pharmacognosy and Phytochemistry, Faculty of Pharmacy, Pancasila University, Jakarta, 12640, Indonesia

[*]Email: sahlan@che.ui.ac.id

Received: 15 Dec 2021, Revised and Accepted: 23 Mar 2022

ABSTRACT

Objective: This study aims to develop a fast, fitted, and accurate classification method for authenticating honey.

Methods: The authentic honey samples were obtained from local beekeepers and distributors, while most of the adulterated honey samples were made from a mixture of fructose syrup, authentic honey, sodium bicarbonate, and sweet soy sauce, while others were received from local distributors. To authenticate the honey, samples were divided into two classes, real honey, and adulterated honey. Similarly, to classify the honey, we categorized two classes, *Apis* spp. and stingless bee. ATR-FTIR spectra data were collected using Thermo Scientific's OMNIC FTIR software and processed using Thermo Scientific's TQ Analyst software by dividing the wavelengths into six regions between 550-4000 cm^{-1}. and Raman spectra data were collected using HORIBA LabSpec 6 software and processed using CAMO's Unscrambler X10.4 software by dividing the Raman shifts into five regions between 200-3350 cm^{-1}.

Results: Our methods effectively authenticate the honey-based on ATR-FTIR and Raman spectra. Based on ATR-FTIR spectra data, the best region of honey's authenticity is Region 1,3,4,5,6 (2800-3000 cm^{-1}; 1640-1760 cm^{-1}; 1175-1455 cm^{-1}; 950-1175 cm^{-1}; 750-950 cm^{-1}) and the best region for classification is 750-950 cm^{-1}. Based on Raman spectra data, the best region of honey's authenticity is 970-1150 cm^{-1} and the best region for classification are 1150-1480 cm^{-1} and 970-1480 cm^{-1}.

Conclusion: This study successfully demonstrated accurate methods based on ATR-FTIR and Raman spectral data to authenticate and classify the honey.

Keywords: Honey, ATR-FTIR, Raman, Discriminant analysis, *Apis* spp., Stingless bee

 DOI: https://dx.doi.org/10.22159/ijap.2022.v14s3.08 Journal homepage: https://innovareacademics.in/journals/index.php/ijap

INTRODUCTION

For a long time, honey is a natural product that has been known for its nutritional value and therapeutic potential [1]. Because of honey's trace nutrients, many people use honey as traditional medicine and food supplements [2]. In Indonesia, the high demand for honey is not matched by its availability. According to the Indonesian Bee Association (API), in 2016–2020, the average demand for honey reaches 15,000 to 150,000 tons per year in Indonesia; whereas, based on the predictions of Dr. James Hutagalung, M. Kes, vice chairman of API, local honey production is only around 15,000 to 75,000 tons per year. In a state of crisis, there are some individuals and companies who adulterated honey with sugar for higher profit margins. Types of honey adulteration include adulterating honey directly by mixing it with common adulterants such as glucose syrup and sucrose syrup, feeding honeybees intensively with sugar, and adulterated honey that is not mixed with real honey [3]. This is a fundamental problem in the market and violates consumers' rights to get the real benefits of honey.

Currently, several methods and parameters can indicate the authenticity of honey, including the measurement of reducing sugar, ash content, 5-hydroxymethylfurfural value (5-HMF), antioxidant activity, and diastase activity [2]. The authenticity of bee products by their botanical origin is typically determined by some methods such as organoleptic analysis, physicochemical methods, and pollen analysis [4]. Whereas the authenticity of bee products by their geographical region is determined by Melissopalynological characterization methods [4]. However, the use of these methods still has some weaknesses, such as being relatively time-consuming, requiring large samples, long-term preparation, and the need for various analytical equipment [2, 4, 5]. In addition, in the previous study, the method of identifying and classifying honey authenticity that had previously been carried out using the ATR-FTIR and chemometric techniques still has a weakness [6]. This method can only identify real honey from two types of adulterated honey. The types of adulterated honey that can be used with this method are adulterated honey mixed with common adulterants and adulterated honey that is formulated without using real honey [6].

This study aims to develop a fast, fitted, and accurate classification method for authenticating honey. Identification and classification of honey authenticity methods will be designed using Discriminant Analysis (DA) methods based on ATR-FTIR and Raman spectroscopy. Raman spectroscopy is a spectroscopic analysis technique in which light scattering is used to produce vibrational spectra of a compound [7]. The advantages of Raman spectroscopy are usable for samples in the form of solids or liquids, no sample preparation, the chemical fingerprint obtained is specific for material, and spectra can be generated quickly in just seconds [8]. The use of chemometrics, especially discriminant analysis techniques is because each compound has different and distinctive FTIR or Raman vibration spectra, so the resulting spectrum may represent the characteristics of a honey sample [9, 10].

MATERIALS AND METHODS

FTIR samples

We used a total of 129 samples consisting of 95 samples of real honey and 34 samples of adulterated honey. Real honey was collected from different geographical regions of Indonesia (19 samples from Sumatera, 50 samples from Java, 20 samples from Kalimantan, 4 samples from Sulawesi, and 2 samples from Irian Jaya) and represented various botanical origins as sources of nectar. Most of the samples were collected directly from beekeepers and distributors. The samples of real honey were produced by *Apis cerana* (n=18), *Apis*

melifera (n=23), *Apis dorsata* (n=29), and stingless bee (n=25). The 25 Adulterated honey samples were made by mixing real honey with water, sucrose, and $NaHCO_3$. And 9 adulterated honey samples were produced by feeding bees intensively with sugar. Honey samples were grouped as either real or adulterated for identification purposes. For classification purposes, the honey samples were labeled as *Apis* spp. and stingless bee.

Raman samples

We used a total of 80 samples consisting of 60 samples of real honey and 20 samples of fake (adulterated) honey. Real honey was collected from different geographical regions of Indonesia and represented various floral origins. Most of the samples were collected directly from primary honey producers. The samples of real honey were produced by *Apis cerana* (n=18), *Apis melifera* (n=23), *Apis dorsata* (n=29), and stingless bee (n=10). The 15 Adulterated honey samples were made by mixing real honey with water, sucrose, and $NaHCO_3$. And 5 the adulterated honey samples were produced by feeding bees intensively with sugar. Honey samples were grouped as either real or adulterated for identification purposes. For classification purposes, the honey samples were labeled as *Apis* spp. and stingless bee.

Chemical and reagent

Sucrose and sodium bicarbonate ($NaHCO_3$) were purchased from Sigma-Aldrich (St. Louis, USA).

ATR-FTIR and Raman spectra measurement

All samples were scanned using Nicolet iS5 FTIR spectrometer (Thermo Fisher Scientific Inc., Waltham, MA, USA) equipped with an iD3 ATR accessory component to produce FTIR spectra. OMNIC software version 9 (Thermo Fisher Scientific Inc., Waltham, MA, USA) was used for collecting the FTIR spectra and spectral data acquisition. Samples were placed on a diamond/ZnSe crystal plate (Thermo Fisher Scientific Inc., Waltham, MA, USA) and scanned at room temperature from 550 to 4000 cm^{-1} for a 16-scan time with a resolution of 16 cm^{-1}. Measurements for each sample were replicated 3 times, and the resulting identical spectra were analyzed. This process was done to evaluate the absorbance value accuracy, which could be affected by sample homogeneity. Propanol was used to clean the diamond between each sample measurement. Meanwhile, to produce Raman spectra, all samples were scanned using HORIBA Micro Confocal Hyperspectral 3D Imaging Raman Spectrometer coupled with excitation laser: 785 nm and gratings 600 gr/mm; the spectrograph allows a resolution of 5 cm^{-1} and scanned from 200 to 3350 cm^{-1}. Data were obtained and analyzed with Horiba's LabSpec 6 software.

Chemometric data analyses

TQ Analyst software (Thermo Fisher Scientific Inc., Waltham, MA, USA) was performed to classify the discriminant analyst model based on FTIR spectral data. In this study, discriminant analysis was used for the determination of spectral differentiation. In this work, discriminant analysis was arranged on ATR-FTIR spectra with the following wavelength ranges: 2800-3000 cm^{-1}, 2400-2200 c cm^{-1}, 1640-1760 cm^{-1}, 1175-1455 cm^{-1}, 950-1175 cm^{-1}, and 750-950 cm^{-1}. Unscrambler X10.4 (CAMO Software, Oslo, Norway) was performed to classify the discriminant analyst model based on Raman spectral data. In this work, discriminant analysis was arranged on Raman spectra with the following Raman shift ranges: 2700–3350 cm^{-1}, 1500–1700 cm^{-1}, 1150–1480 cm^{-1}, 970–1150 cm^{-1}, and 300–950 cm^{-1}.

RESULTS

Analysis of ATR-FTIR spectra

Fig. 1 shows the results of ATR-FTIR spectrum of real (blue line) and adulterated honey (red line) samples, which are divided into six specific spectral regions from 500 to 4000 cm^{-1}. Table 1 shows the band assignments in conjunction with corresponding modes of vibration in the ATR-FTIR spectrum of honey, based on Gok, 2014 and the literature [11, 12]. The specific peaks and shoulders on ATR-FTIR spectrum of real honey 550–4000 cm^{-1} are demonstrated in fig. 2.

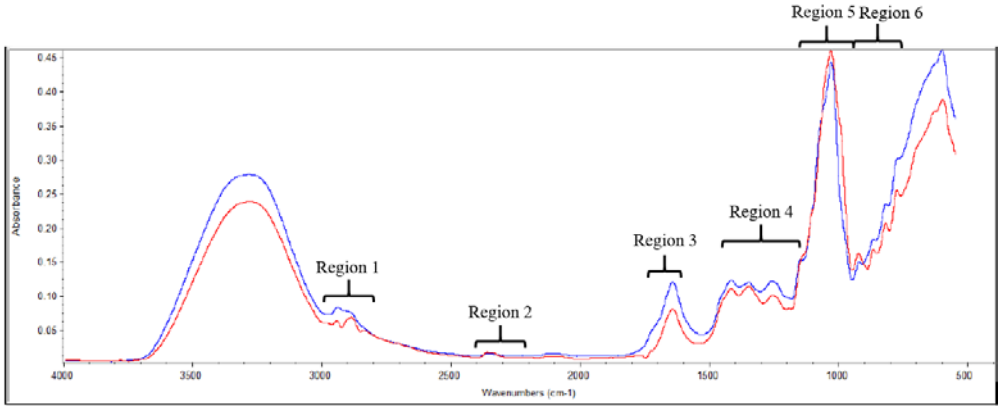

Fig. 1: ATR-FTIR spectra of pure honey and also of adulterated honey in 550–4000 cm^{-1}

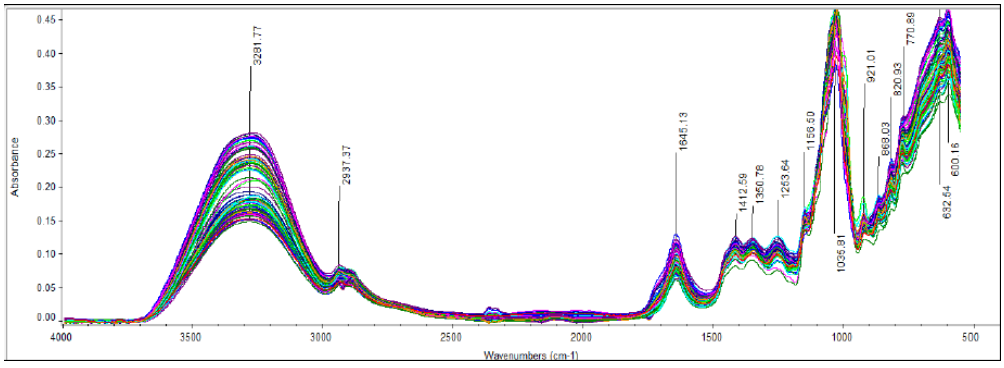

Fig. 2: The specific peaks on ATR-FTIR spectrum of real honey in 550–4000 cm^{-1}

Table 1: General band assignment of ATR-FTIR spectrum of honey

Region 1	2800–3000 cm^{-1}	C-H stretching (carbohydrates) O-H stretching (carboxylic acids) NH_3 stretching (free amino acids)
Region 2	2400–2200 cm^{-1}	CO_2 stretching (carbohydrate decomposition)
Region 3	1640–1760 cm^{-1}	O-H stretching/bending (water) C=O stretching (mainly from carbohydrates) N-H bending of amide I (mainly proteins)
Region 4	1175–1455 cm^{-1}	O-H stretching/bending C-H stretching (carbohydrates) C=O stretching of ketones
Region 5	950–1175 cm^{-1}	C-O and C-C stretching (carbohydrates) Ring vibrations (mainly from carbohydrates)
Region 6	750–950 cm^{-1}	Anomeric region of carbohydrates C-H bending (mainly from carbohydrates) Ring vibrations (mainly from carbohydrates)

Discriminant analysis based on ATR-FTIR spectra

Regional selection was conducted based on observing the results of the honey ATR-FTIR spectrum. For authentication study, samples are divided into two classes, real honey, and adulterated honey. The chemometrics of DA was applied to the authentication and classification of honey by using the different spectral regions, as shown in table 2. The results in table 2 indicates that the best authentication of honey was obtained in region 1,3,4,5,6 (2800–3000 cm^{-1}, 1640–1760 cm^{-1}, 1175–1455 cm^{-1}, 950–1175 cm^{-1}, and 750–950 cm^{-1}) with 95.1 performance index and there are not any misclassification samples.

The best DA results are revealed in fig. 3 which indicates two separating groups between real honey and adulterated honey. The real honey spectrum is indicated by the square symbols and the adulterated honey spectrum is indicated by the triangle symbols, as shown in fig. 3.

Table 2: Effect of selected spectra region for authentication of honey

Wavelength (cm^{-1})	Performance index	Misclassified	Total samples
4000–550	87.0	5	129
Region 1 (2800–3000)	89.1	4	129
Region 2 (2400–2200)	81.0	9	129
Region 3 (1640–1760)	90.0	1	129
Region 4 (1175–1455)	90.4	-	129
Region 5 (950–1175)	86.7	15	129
Region 6 (750–950)	85.7	10	129
Region 1–6	91.6	-	129
Region 2–6	90.8	3	129
Region 3–6	91.1	2	129
Region 4–6	90.8	2	129
Region 1,3,4,5,6	95.1	-	129
750–550	82.3	21	129

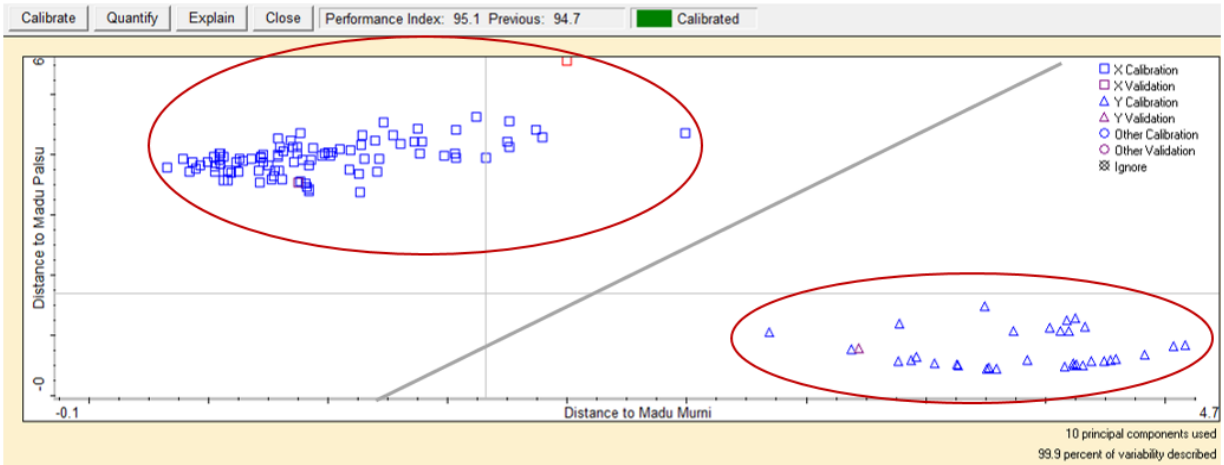

Fig. 3: Discriminant analysis scatter plots for authentication honey in the region 1,3,4,5,6 (2800–3000 cm^{-1}, 1640–1760 cm^{-1}, 1175–1455 cm^{-1}, 950–1175 cm^{-1}, and 750–950 cm^{-1})

For the classification study, the samples are categorized into two classes by types of honeybees, *Apis* spp. and stingless bee. The results of DA using TQ Analyst software are shown in table 3. It shows that the best classification of honey was obtained in region 6 (750–950 cm^{-1}). When we use region 6 only, the performance index is 94.9 and no samples were misclassified. The *Apis* spp. honey spectra are indicated by the square symbols and the stingless bee honey spectra are indicated by the triangle symbols, as shown in fig. 4.

Table 3: Effect of selected spectra region for classification of honey

Wavelength (cm^{-1})	Performance index	Misclassified	Total samples
4000–550	91.5	2	95
Region 1 (2800–3000)	94.3	-	95
Region 2 (2400–2200)	81.6	21	95
Region 3 (1640–1760)	92.5	-	95
Region 4 (1175–1455)	94.4	-	95
Region 5 (950–1175)	93.9	-	95
Region 6 (750–950)	94.9	-	95
Region 1–6	93.9	-	95
Region 2–6	94.0	-	95
Region 3–6	94.2	-	95
Region 4–6	94.2	-	95
Region 1,3,4,5,6	93.7	-	95
750–550	91.7	1	95

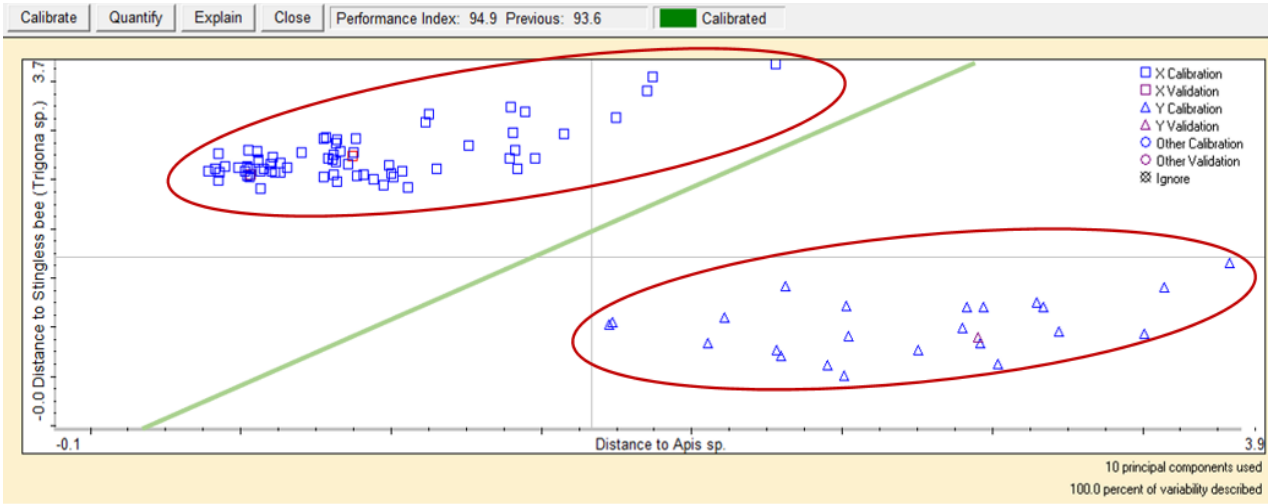

Fig. 4: Scatter plots for classification of honey based on 2 types of honey bees at 950–750 cm^{-1}

Analysis of Raman spectra

The results of Raman spectrum of real (blue line) and adulterated (red line) honey samples are shown in fig. 5. In fig. 5, the spectrum is divided into five specific spectral regions from 200 to 3350 cm^{-1}. Table 4 shows the band assignments in conjunction with corresponding modes of vibration in the Raman spectrum of honey, based on the literature [11, 13-15]. The specific peaks and shoulders on the Raman spectrum of real honey 200–3350 cm^{-1} are demonstrated in fig. 6.

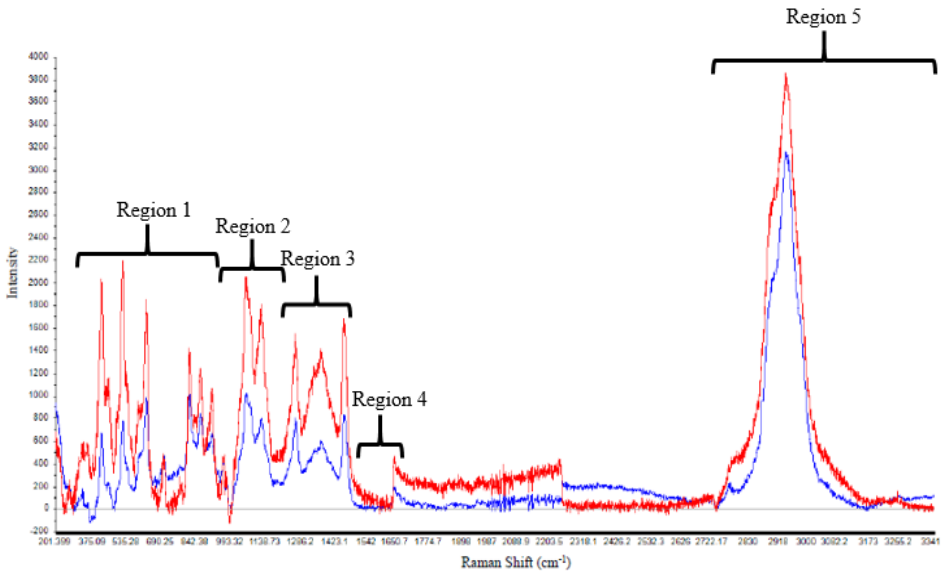

Fig. 5: Raman spectra of pure honey and also of adulterated honey in 200–3350 cm^{-1}

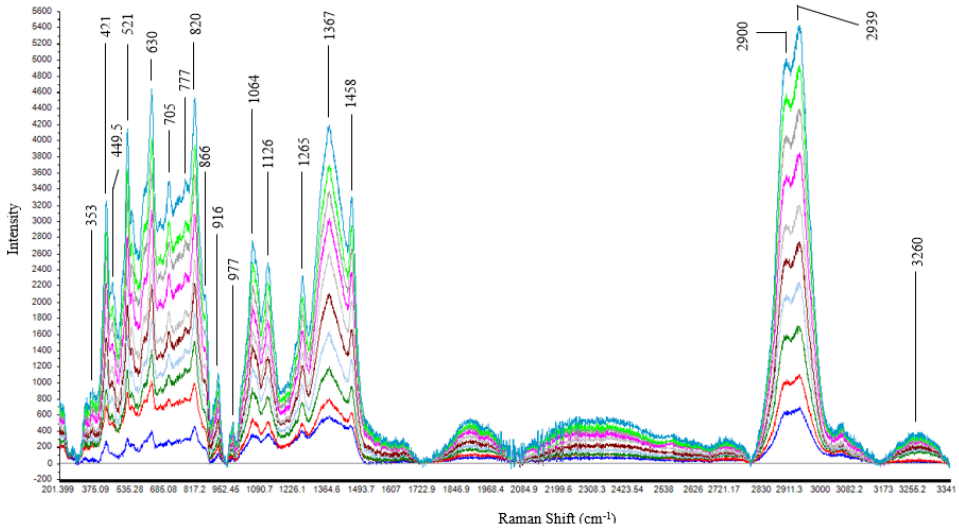

Fig. 6: The specific peaks on Raman spectrum of real honey in 200–3350 cm^{-1}

Table 4: General band assignment of Raman spectrum of honey

Region 1	300–950 cm^{-1}	C-H and C-O-H deformation Ring deformation Plane deformation C-C-O and C-C-C deformation
Region 2	970–1150 cm^{-1}	C-O stretching C-O-H deformation; C-N vibration (protein or amino acid)
Region 3	1150–1480 cm^{-1}	C-C-H, O-C-H and C-O-H deformation; Amide III vibration (peptide bond) Asymmetric CH_2 deformation
Region 4	1500–1700 cm^{-1}	O–H deformation in water
Region 5	2700–3350 cm^{-1}	C-H stretching Asymmetric CH_2 stretching O–H stretching

Discriminant analysis based on Raman spectra

DA have been applied to different spectral regions using Unscrambler X10.4 software. The results of DA based on the Raman spectrum are shown in table 5. Similar to DA based on ATR-FTIR spectra, for the identification study, the samples are divided into two classes, real honey, and adulterated honey. The results in table 5 indicate that the best authentication of honey was obtained in region 2 (970–1150 cm^{-1}) with 100% grouping accuracy and no samples were misclassified.

The result of the best authentication of honey is shown in fig. 7. It shows the classification of honey based on its authenticity, real honey (blue) and adulterated honey (red) separated by using a black line.

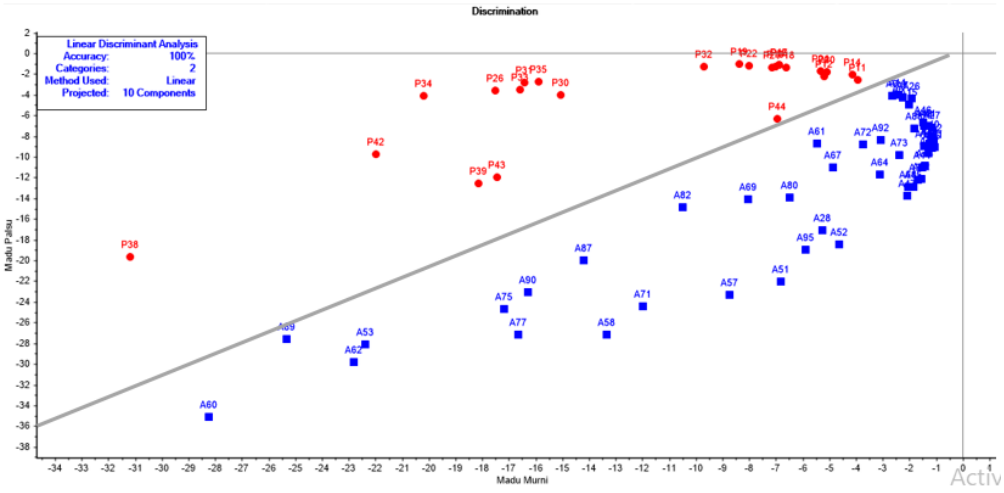

Fig. 7: The results of honey authenticity in region 2 (970–1150 cm^{-1})

Similar to DA based on ATR-FTIR spectra, for classification study, samples are separated into two classes, *Apis* spp. Honey and stingless bee honey. To classify the honey, the Raman spectrum was analyzed using the DA method on Unscrambler X10.4 software and

the results of DA are shown in table 6. Based on the results in table 6, the best classification was obtained in region 3 (1150–1480 cm^{-1}) and regions 2-3 (970–1150 cm^{-1} and 1150–1480 cm^{-1}) with 100% grouping accuracy and no samples were misclassified.

The result of the best classification of honey is shown in fig. 8. Fig. 8 shows the classification of honey-based on types of honey-bees, stingless bee honey (blue), and *Apis* spp. honey (red) is separated by using a green line.

Table 5: Effect of selected scattering spectra region for authentication of honey

Raman shift (cm^{-1})	Accuracy	Misclassified	Total samples
200–3350	86.49%	10	80
Region 1 (300–950)	90.54%	7	80
Region 2 (970–1150)	100%	-	80
Region 3 (1150–1480)	94.59%	4	80
Region 4 (1500–1700)	90.54%	7	80
Region 5 (2700–3350)	98.65%	1	80
Region 1–3	91.89%	6	80
Region 1–4	86.49%	10	80
Region 1–5	87.84%	9	80
Region 1, 2, 3, 5	93.24%	5	80

Table 6: Effect of selected scattering spectra region for classification of honey

Raman shift (cm^{-1})	Accuracy	Misclassified	Total Samples
200–3350	92.42%	5	60
Region 1 (300–950)	98.48%	1	60
Region 2 (970–1150)	96.97%	2	60
Region 3 (1150–1480)	100%	-	60
Region 4 (1500–1700)	96.97%	2	60
Region 5 (2700–3350)	98.48%	1	60
Region 1–3	98.48%	1	60
Region 2–3	100%	-	60
Region 1-4	98.48%	1	60
Region 1–5	96.97%	2	60
Region 1, 2, 3, 5	95.45%	3	60

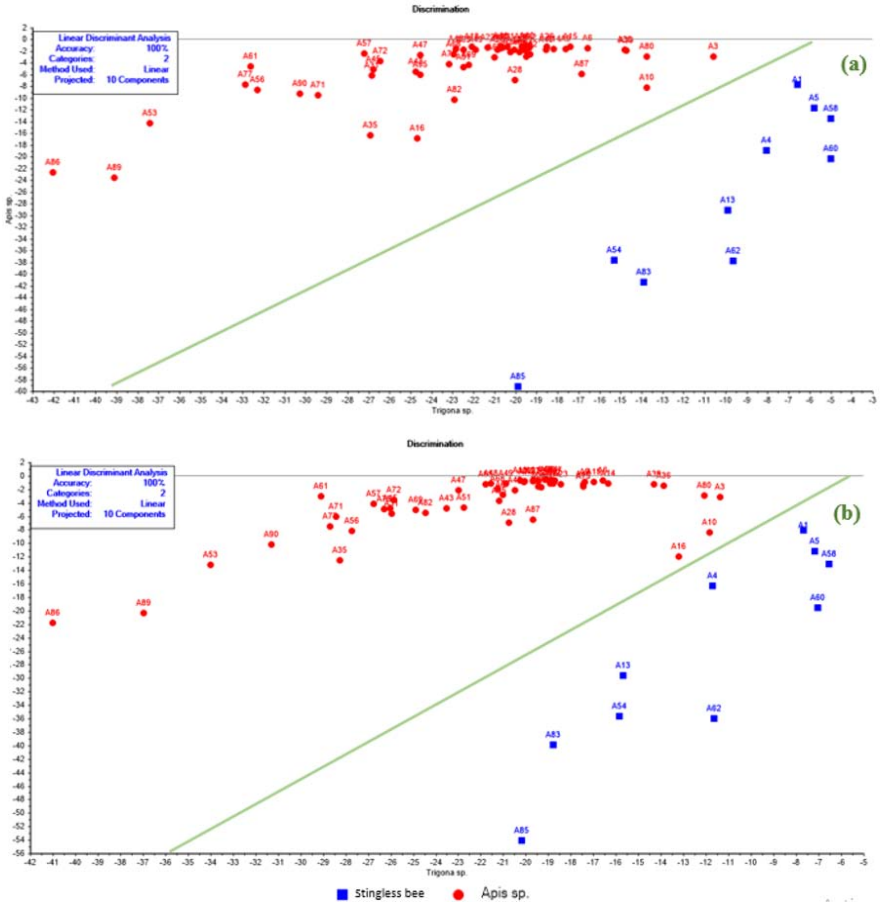

Fig. 8: The results of the honey classification based on two classes of bee-producing bees in, (a) Region 3 (1150–1480 cm^{-1}), (b) Region 2–3 (970–1480 cm^{-1})

DISCUSSION

Comparison between ATR-FTIR and Raman spectra

The information of nutritional value obtained from ATR-FTIR and Raman spectra is similar to the previous studies, which determine main carbohydrates (sucrose, fructose, glucose) and estimated the content of phenolic compounds and antioxidant activity in honey [6, 28].

The basic principle of FTIR and Raman spectroscopy is measuring the interaction of energy with the light that can excite vibrational transitions of molecular bonds in a sample but differ in some fundamental ways. In Raman spectroscopy, the active vibration depends on a change in polarizability of a molecule (focuses on scattering of light by the vibrating molecules), whereas the active vibration in ATR-FTIR spectroscopy depends on a change in dipole moment (focuses on absorption of light by the vibrating molecules) [16]. Honey spectra were obtained using ATR-FTIR and Raman spectroscopy. The ATR-FTIR spectra show the spectral peaks in the 550–4000 cm^{-1} region and 200–3350 cm^{-1} region for Raman spectra.

Based on the characteristics, ATR-FTIR spectroscopy is sensitive to functional group vibration and polar bonds, mainly OH stretching in water (strong peak at 3292 cm^{-1}). Water can absorb the light greatly and affect the infrared spectra [16]; whereas in the Raman spectra, very weak peaks at 1600–1700 cm^{-1} could be associated with the OH from water. This is probably because water with small single bonds tends to be a very weak scatterer of Raman.

Honey has intrinsic emission properties, which are probably associated with the mixture of fluorophores such as amino acids, vitamins, and polyphenols [17]. The fluorescence of honey can interfere with the Raman spectra. The fluorescence follows an absorption process that causes molecules to be excited to a higher electronic state which has the high energy required for this process. If fluorescence is raised, it can be more intense than Raman scattering and hiding Raman features [17, 18]. Because of the fluorescence, 49 honey spectrum measured by Raman spectroscopy can't be used for discriminant analysis.

Authentication and classification of honey using discriminant analysis based on ATR-FTIR spectra data

The results of this research indicated the capability prospect of ATR-FTIR spectroscopy in collaboration with DA as an automated and greatly sensitive method to divided honey samples into two groups, real honey, and adulterated honey. This method also showed the potential capability methods for classifying honey samples based on their types of honeybees, *Apis* spp., and stingless bee [19]. In this study, ATR-FTIR spectroscopy was applied to compare honey samples based on their spectral differences in the wavelength between 550 to 4000 cm^{-1}. The crystal used in the ATR cells is made from materials that have a low solubility in water and a remarkably high refractive index [20].

The DA method based on ATR-FTIR spectra successfully identified and classified the honey samples [20]. For identification of honey's authenticity, the results are shown that the best authentication was obtained in region 1,3,4,5,6 (2800–3000 cm^{-1}, 1640–1760 cm^{-1}, 1175–1455 cm^{-1}, 950–1175 cm^{-1}, and 750–950 cm^{-1}) with a performance index 94.7 and no samples were misclassified. The peak was observed at regions 3-6 which are more sensitive to the main component of honey, carbohydrates (about 60-75%). At wavenumbers of 750–1500 cm^{-1} shows the characteristics of the three major sugar content in honey: sucrose, glucose, and fructose [21]. The peaks observed at 750–900 cm^{-1} could be associated with the characteristic and anomeric region of saccharide configurations. The peaks observed at a wavelength of 1640–1760 cm^{-1} may be because of the C=O stretching mainly from carbohydrates and H-O-H stretching [10]. The peak observed at 2800–3000 $cm^{-1,}$ which strongly shows at 2937 cm^{-1} could be associated with the presence of C-H stretching from carboxylic acids and NH_3 stretching from free amino acids [19]. This information could be associated with the content of phenolic compounds in honey.

Based on the results, the best classification was obtained at the wavelength of 750–950 cm^{-1} with a 94.9 performance index and no samples were misclassified when we use the region. The range of wavelength between 750 and 950 cm^{-1} indicates the presence of C-C stretching and C-H bending in the carbohydrate structure [11]. The peak observed in this region may also be because of saccharide configuration or anomeric group on carbohydrates. Based on this information, the classification of honey produced by *Apis* spp. and stingless bees can be distinguished based on their carbohydrate or sugar content. According to Amin *et al.*, (2018), the honey produced by *Trigona* sp. has a lower sucrose content when compared to honey produced by *Apis dorsata* and *Apis mellifera*. Honey produced by stingless bees or *Trigona* sp. had sucrose content ranging from 0.31 to 1.26 w/w, while honey produced by *Apis dorsata* and *Apis melifera* had sucrose content of 0.6 w/w and 2.8 w/w [22]. The results of data processing also show 94.4 high-performance indexes in the range of wavelength from 1175 to 1455 cm^{-1}. The wavelength 1175–1455 cm^{-1} could be associated with the O-H, C-H, and C=C bending, which may be related to the flavanol and phenol content in honey. Previous studies have compared the antioxidant activity of honey produced by stingless bees with honey produced by stinging bees. Martinello and Mutinelli (2021) have mentioned in their research that honey produced by the stingless bee, *Melipona beecheii*, showed higher levels of total antioxidants, flavonoids, carotenoids, ascorbic acid, free amino acids, and protein when compared to honey produced by *Apis mellifera*. The honey produced by *Trigona* sp. Also has a higher total phenol content when compared to honey produced by *Apis* spp [23].

Authentication and classification of honey using discriminant analysis based on Raman spectra data

Raman spectroscopy is based on the inelastic scattering of light passing through a sample. This light scattering means that the energy of the photon will shift after interacting with the molecules in the sample. This energy shift produces information about vibrations, rotations, or energy transitions into the sample molecules [24]. The advantages of Raman spectroscopy are non-destructive, can be used for direct analysis, does not require any sample preparation, the presence of water solvent will not interfere with the Raman spectrum, and organic or inorganic compounds can be used as samples. With Raman, the acquisition of a single spectrum can be fast, where a single Raman spectrum can be obtained in the time range of 0.1-10 seconds, depending on the sensitivity of the system [25, 26].

For authentication of honey, the results are shown that the best identification was obtained in region 2 (970–1150 cm^{-1}) with 100% grouping accuracy and no samples were misclassified. Each peak and shoulder on Raman spectra at Raman shift of 970–1150 cm^{-1} shows the characteristics of the three main sugar content in honey: sucrose, glucose, and fructose. The small peak at 977 cm^{-1} could be associated with the presence of vibrations in the two anomers of fructose and glucose [2]. The peak observed at 1064 cm^{-1} may be because of C-O stretching on the glucose ring as seen in the spectra of glucose, maltose, and sucrose. The peak viewed at Raman Shifts of 1074–1077 cm^{-1} could be associated with the deformation of the C-O-H group from glucose and glucose. The peaks may also indicate the minor effect of the vibration of the C-N group on proteins or amino acids [8].

For the classification of honey based on the types of honeybees, the results are shown that the best classification was obtained in region 3 (1150–1480 cm^{-1}) and region 2-3 (970–1150 cm^{-1} and 1150–1480 cm^{-1}) with 100% grouping accuracy and no samples were misclassified. Each peak and shoulder on Raman spectra at Raman shift 1150–1480 cm^{-1} shows their presence in the 1265 cm^{-1}, 1367 cm^{-1} and 1458 cm^{-1}. The peak observed at 1265 cm^{-1} could be associated with the deformation of C-C-H, C-O-H, and O-C-H groups, which may be related to the presence of phenolic compounds in honey. According to the research by Pompeu *et al.*, (2018), phenolic compounds such as gallic acid, 4-hydroxybenzoic acid, and syringic acid showed strong spectral peaks at 1260–1266 cm^{-1}. These peaks could be associated with the deformation vibrations inside and outside the plane of the =C-H aromatic group. A strong peak observed at 1367 cm^{-1} could be associated with the bending of the C-H and O-H groups. The peak observed at Raman shifts of 1310–1410

cm^{-1} maybe because of the deformation of the O-H group and the stretching of the C-O group on phenol [28]. The peak seen at 1458 cm^{-1} could indicate the vibrations of the COO-group from the bending of the CH_2 group. This peak could also be associated with the presence of flavanols and organic acids in honey [29].

In region 2, there are quite strong spectral peaks at the Raman Shift 977 cm^{-1}, 1064 cm^{-1}, and 1126 cm^{-1}. The Raman shift 977 cm^{-1} indicates the presence of vibrations in both fructose and glucose anomers. This Raman shift can also be attributed to the presence of a bend in the C-H group. The peak seen in the 1064-1077 cm^{-1} scattering region indicates the presence of C-O group stretching, bending of C-H and C-O-H group, especially in carbohydrates, and can also be associated with the presence of C-N group vibrations in amino acids and proteins. The peak seen in the 1126 cm^{-1} scattering region indicates a bend in the C-H group. The Raman shifts of 970–1150 cm^{-1} could also be associated with the combination stretching of C-O and C-O-C and also C-N vibrations in proteins and amino acids [9, 29, 30].

CONCLUSION

We suggest the methods rapidly and accurately for authentication and classification of honey using discriminant analysis based on ATR-FTIR and Raman spectra data. This method successfully demonstrated to the grouping of the authentication and classification of honey-based on the honey's spectrum.

ACKNOWLEDGMENT

The author gratefully acknowledged the Basic Chemical Process Laboratory Faculty of Engineering University of Indonesia and the Integrated Laboratory and Research Center (ILRC) the University of Indonesia who has provided facilities for this research.

FUNDING

This research was funded by the Indonesian Ministry of Research and Technology/National Agency for Research and Innovation and Indonesian Ministry of Education and Culture under Program Penelitian Kolaborasi Indonesia (PPKI) 2021 managed by Universitas Indonesia, contract no. NKB-462/UN2. RST/HKP.05.00/ 2021.

AUTHORS CONTRIBUTIONS

NALA, AA, AS, DKP, and MS: Arranged, designed, and supervised the study. AA, AS and NALA: Collected honey samples for the study. NALA: Carried out sampling and laboratory analysis and wrote the first draft of the manuscript. NALA: Analyzed the data. MS, NALA, and DKP: Contributed to the writing of the manuscript. DKP and MS: Jointly developed the structure and arguments for the paper. DKP and MS: Made critical revisions. All authors read and approved the final manuscript.

CONFLICT OF INTERESTS

The authors declare that they have no competing interests.

REFERENCES

1. Meo SA, Al-Asiri SA, Mahesar AL, Ansari MJ. Role of honey in modern medicine. Saudi J Biol Sci. 2017;24(5):975-8. doi: 10.1016/j.sjbs.2016.12.010, PMID 28663690.
2. Ahmed S, Sulaiman SA, Baig AA, Ibrahim M, Liaqat S, Fatima S. Honey as a potential natural antioxidant medicine: an insight into its molecular mechanisms of action. Oxid Med Cell Longev. 2018;2018:8367846. doi: 10.1155/2018/8367846. PMID 29492183.
3. Johari NA, Ashaari NS, Mamat MR, Muhamad A. Simple and rapid screening test to detect fake honey product. J Agric Sci Technol. 2019;9:330-8.
4. Ruoff K, Bogdanov S. Authenticity of honey and other bee products. Apiacta. 2004;38:317-27.
5. Cozzolino D, Corbella E, Smyth HE. Quality control of honey using infrared spectroscopy: a review. Appl Spectrosc Rev. 2011;46(7):523-38. doi: 10.1080/05704928.2011.587857.
6. Sahlan M, Karwita S, Gozan M, Hermansyah H, Yohda M, Yoo YJ. Identification and classification of Honey's authenticity by attenuated total reflectance fourier-transform infrared spectroscopy and chemometric method. Vet World. 2019;12(8):1304-10. doi: 10.14202/vet world.2019.1304-1310, PMID 31641312.
7. Hassing S. What is vibrational raman spectroscopy: A vibrational or an electronic spectroscopic technique or both? Modern spectroscopic techniques and applications. In: Khan M, Morari DNG, El-Azazy M, editors. Modern spectroscopic techniques and applications. London, United Kingdom: IntechOpen; 2020. p. 13-38.
8. Oroian M, Ropciuc S, Paduret S. Honey adulteration detection using Raman spectroscopy. Food Anal Methods. 2018;11(4):959-68. doi: 10.1007/s12161-017-1072-2.
9. Pierna JA, Abbas O, Dardenne P, Baeten V. Discrimination of corsican honey by FT-Raman spectroscopy and chemometrics. Biotechnol Agron Soc Environ. 2011;15:75-84.
10. Damiani T, Alonso Salces RM, Aubone I, Baeten V, Arnould Q, Dall'Asta C. Vibrational spectroscopy coupled to a multivariate analysis tiered approach for argentinean honey provenance confirmation. Foods. 2020;9(10):1450. doi: 10.3390/ foods9101450, PMID 33066066.
11. Gok S, Severcan M, Goormaghtigh E, Kandemir I, Severcan F. Differentiation of Anatolian honey samples from different botanical origins by ATR-FTIR spectroscopy using multivariate analysis. Food Chem. 2015;170:234-40. doi: 10.1016/j.foodchem.2014.08.040, PMID 25306340.
12. Liu Z, Qi N, Luan Y, Sun X. Thermogravimetry-infrared spectroscopy analysis of the pyrolysis of willow leaves, stems, and branches. Adv Mater Sci Eng. 2015;2015:1-8. doi: 10.1155/2015/303212.
13. Salvador L, Guijarro M, Rubio D, Aucatoma B, Guillen T, Vargas Jentzsch P. Exploratory monitoring of the quality and authenticity of commercial honey in ecuador. Foods. 2019;8(3):105. doi: 10.3390/foods8030105, PMID 30897757.
14. Ilaslan K, Boyaci IH, Topcu A. Rapid analysis of glucose, fructose and sucrose contents of commercial soft drinks using Raman spectroscopy. Food Control. 2015;48:56-61. doi: 10.1016/j.foodcont.2014.01.001.
15. Goodacre R, Radovic BS, Anklam E. Progress toward the rapid, nondestructive assessment of the floral origin of European honey using dispersive Raman spectroscopy. Appl Spectrosc. 2002;56(4):521-7. doi: 10.1366/0003702021954980.
16. Anjos O, Guine RPF, Santos AJA, Paula VB, Pereira H, Estevinho LM. Evaluation of FT-Raman and FTIR-ATR spectroscopy for the quality evaluation of Lavandula spp. honey. Open Agric. 2021;6(1):47-56. doi: 10.1515/opag-2020-0210.
17. Lenhardt L, Bro R, Zekovic I, Dramicanin T, Dramicanin MD. Fluorescence spectroscopy coupled with PARAFAC and PLS DA for characterization and classification of honey. Food Chem. 2015;175:284-91. doi: 10.1016/j.foodchem.2014.11.162, PMID 25577082.
18. Ishikawa Ankerhold HC, Ankerhold R, Drummen GP. Advanced fluorescence microscopy techniques—FRAP, flip, Flap, fret and Flim. Molecules. 2012;17(4):4047-132. doi: 10.3390/molecules17044047, PMID 22469598.
19. Anjos O, Campos MG, Ruiz PC, Antunes P. Application of FTIR-ATR spectroscopy to the quantification of sugar in Honey. Food Chem. 2015;169:218-23. doi: 10.1016/j.foodchem.2014.07.138, PMID 25236219.
20. Andrew Chan KL, Kazarian SG. Attenuated total reflection fourier-transform infrared (ATR-FTIR) imaging of tissues and live cells. Chem Soc Rev. 2016;45(7):1850-64. doi: 10.1039/c5cs00515a, PMID 26488803.
21. Kędzierska Matysek M, Matwijczuk A, Florek M, Barłowska J, Wolanciuk A, Matwijczuk A. Application of FTIR spectroscopy for analysis of the quality of Honey. BIO Web Conf. 2018;10:02008. doi: 10.1051/bioconf/20181002008.
22. Zulkhairi Amin FA, Sabri S, Mohammad SM, Ismail M, Chan KW, Ismail N. Therapeutic properties of stingless bee honey in comparison with European bee honey. Adv Pharmacol Sci. 2018;2018:6179596. doi: 10.1155/2018/6179596, PMID 30687402.
23. Martinello M, Mutinelli F. Antioxidant activity in bee products: a review. Antioxidants (Basel). 2021;10(1):71. doi: 10.3390/antiox10010071, PMID 33430511.

24. Smith E, Dent G. Modern raman spectroscopy: a practical approach. Hoboken, United States. J Wiley Andamp Sons; 2008.
25. Ember KJI, Hoeve MA, McAughtrie SL, Bergholt MS, Dwyer BJ, Stevens MM. Raman spectroscopy and regenerative medicine: a review. NPJ Regen Med. 2017;2:12. doi: 10.1038/s41536-017-0014-3, PMID 29302348.
26. Mitsutake H, Poppi R, Breitkreitz M. Raman imaging spectroscopy: history, fundamentals and current scenario of the technique. J Braz Chem Soc. 2019;30:2243-58. doi: 10.21577/0103-5053.20190116.
27. Mathlouthi M, Vinh Luu D. Luu D. Laser-raman spectra of D-glucose and sucrose in aqueous solution. Carbohydrate Research. 1980;81(2):203-12. doi: 10.1016/S0008-6215(00)85652-9.
28. Pompeu DR, Larondelle Y, Rogez H, Abbas O, Pierna JAF, Baeten V. Characterization and discrimination of phenolic compounds using Fourier transform Raman spectroscopy and chemometric tools. Biotechnol Agron Soc Environ. 2018;22:13-28. doi: 10.25518/1780-4507.16270.
29. Anjos O, Santos AJA, Paixao V, Estevinho LM. Physicochemical characterization of Lavandula spp. honey with FT-Raman spectroscopy. Talanta. 2018;178:43-8. doi: 10.1016/j.talanta.2017.08.099, PMID 29136844.
30. Aguilar Hernandez I, Afseth NK, Lopez Luke T, Contreras Torres FF, Wold JP, Ornelas Soto N. Surface-enhanced raman spectroscopy of phenolic antioxidants: A systematic evaluation of ferulic acid, P-coumaric acid, caffeic acid and sinapic acid. Vib Spectrosc. 2017;89:113-22. doi: 10.1016/j.vibspec.2017.02.002.